

6. Atmospheric (Ozone) chemistry model (MRI-CCM2)

Tropospheric ozone is a major greenhouse gas now ranked third following CO₂ and CH₄ (IPCC-AR4, 2007), whereas the destruction of stratospheric ozone during the most recent several decades by man-made ozone-depleting gases such as CFCs potentially increases surface ultraviolet radiation (e.g., WMO/UNEP, 2007) and impacts on the earth's climate (e.g., Son et al., 2008), especially over the Southern extra-tropics. The increase in photochemical oxidants near the earth's surface since the industrial era can also harm humans and vegetation. A CCM for predicting global distributions of atmospheric trace gases such as ozone along with chemistry–climate interactions is an invaluable tool for addressing these environmental issues. A CCM developed at MRI (Deushi and Shibata, 2010; Shibata et al., 2005) called MRI-CCM2 is incorporated into MRI-ESM1 as a component model to evaluate the impacts of changes in ozone and other trace gases on the earth's climate. The target region of MRI-CCM2 is from the surface to the upper stratosphere. In MRI-ESM1, concentrations of radiatively active gases (ozone, CH₄, N₂O, and CFCs) calculated by MRI-CCM2 are used in the AGCM radiation module to consider chemistry–radiation coupling processes. Chemical coupling processes between trace gases and aerosols can also be considered, wherein MRI-CCM2 takes into account heterogeneous reactions on sulfate and sea-salt aerosol surfaces using concentrations predicted by the MASINGAR mk-2 aerosol model. MRI-CCM2 simulates the following processes: chemical conversion of trace gases, (grid-scale) advective transport, (sub-grid-scale) convective transport and boundary-layer diffusion, dry and wet deposition, and emissions. MRI-CCM2 incorporates a detailed tropospheric ozone chemical mechanism, which includes elaborate HO_x-NO_x-CH₄-CO photochemistry and a near-explicit degradation mechanism of nonmethane hydrocarbons (NMHCs), and a major stratospheric ozone chemical mechanism that treats heterogeneous reactions on type I and II polar stratospheric clouds and sulfate aerosols as well as gas-phase reactions. In all, MRI-CCM2 includes 90 chemical species and treats 243 chemical reactions: 168 gas-phase reactions, 59 photochemical reactions, and 16 heterogeneous reactions. A hybrid semi-Lagrangian transport scheme is used for chemical species, in which the advection equation is solved with the mass conservation equation. Emissions of NO_x, CH₄, CO, NMHCs, N₂O, CFCs, and halons include sources from industry, biomass burning, vegetation, soil, ocean, aircraft, lightning, and cosmic rays.

The seasonal cycle of the zonal-mean total ozone during 1978–1980 simulated by MRI-ESM1 as a function of months is compared with observation in Figure 11. The observed ozone is from satellite measurements by the total ozone mapping spectrometer (TOMS) and solar backscattered ultraviolet (SBUV) (TOMS/SBUV merged total and profile ozone data sets based on the version 8 retrieval algorithm; http://code916.gsfc.nasa.gov/Data_services/merged). The model generally captures well the observed features of the total ozone distribution. In the tropics, the simulated total ozone shows little bias throughout the year and the seasonal cycle is fairly well reproduced. The model also simulates the observed seasonal march in the northern extratropics, where a high-latitude total ozone maximum occurs in the late winter and early spring. In the southern mid-latitudes, however, positive biases of several tens of Dobson units (DU) are simulated from winter to spring. Figure 12 illustrates latitude–pressure cross sections of observed and simulated zonal-mean ozone volume mixing ratios in the stratosphere for January and July. The observations for 1978–1985 are based on SBUV satellite data, which cover the middle atmosphere from 50 to about 0.3 hPa. The model reproduces well the ozone core region in the equatorial upper stratosphere centered at 10 hPa, although it slightly underestimates the volume mixing ratio by up to 1 ppmv. The simulated and observed annually averaged zonal-mean ozone in the troposphere during the 1990s are shown in Figure 13. The simulated tropospheric ozone quantitatively captures observed features such as tropical low ozone mixing ratios near the surface extending upward due to intensive convective activity and sharp vertical gradients in the extratropics that approximately parallels the tropopause.

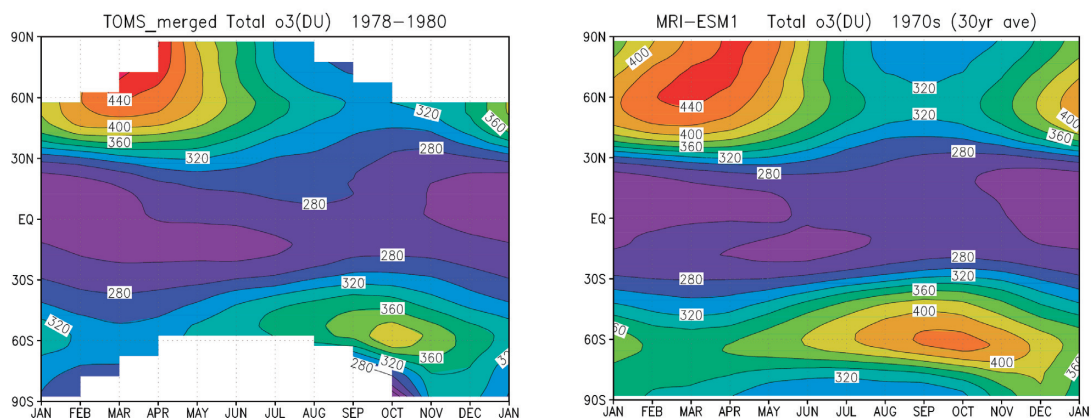


Figure 11 Month-latitude cross sections of the zonal-mean total ozone (in DU) for TOMS/SBUV observation averaged over the period of 1978–1980 (left) and the 1970s climatology of the MRI-ESM1 simulation (right). Contour interval is 20 DU.

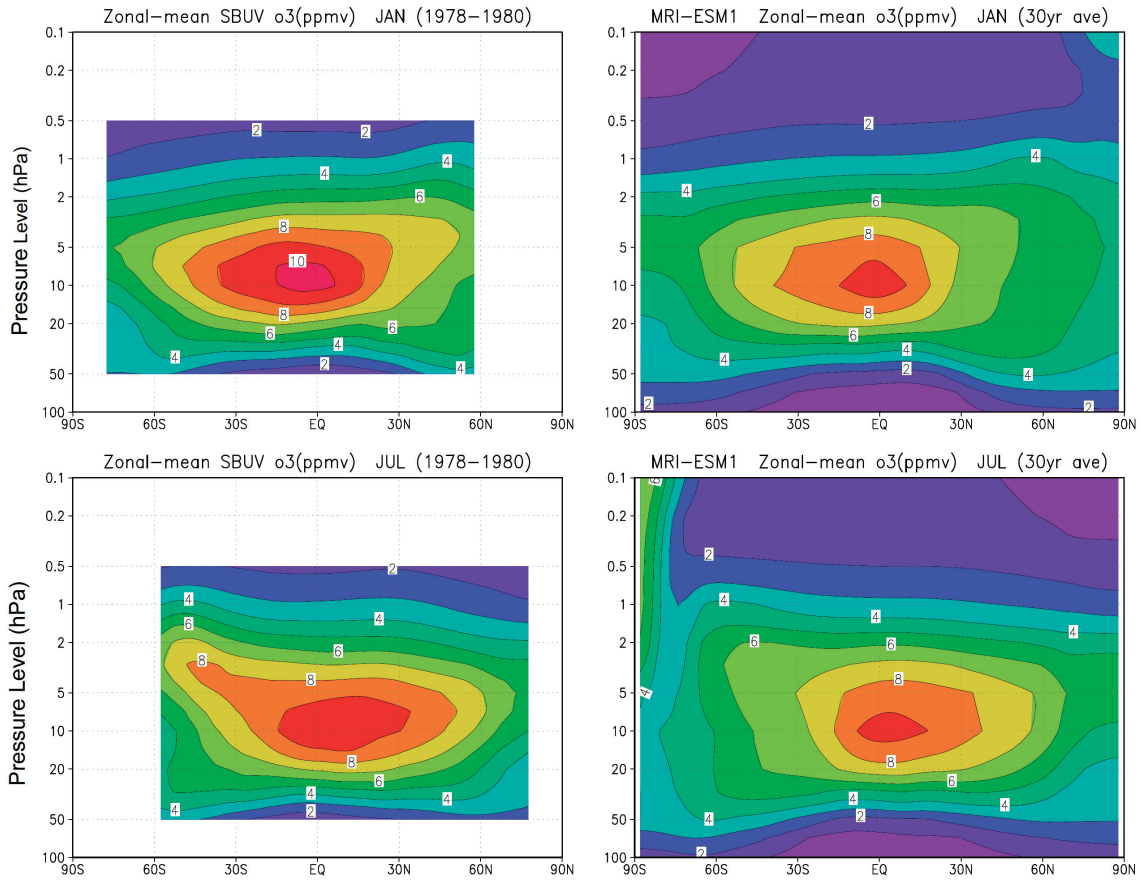


Figure 12 Latitude-pressure cross section of zonal-mean stratospheric ozone mixing ratios (in ppmv) in January (upper) and July (lower) for SBUV observation averaged over the period of 1978-1980 (left) and the 1970s climatology of the MRI-ESM1 simulation (right). Contour interval is 1 ppmv.

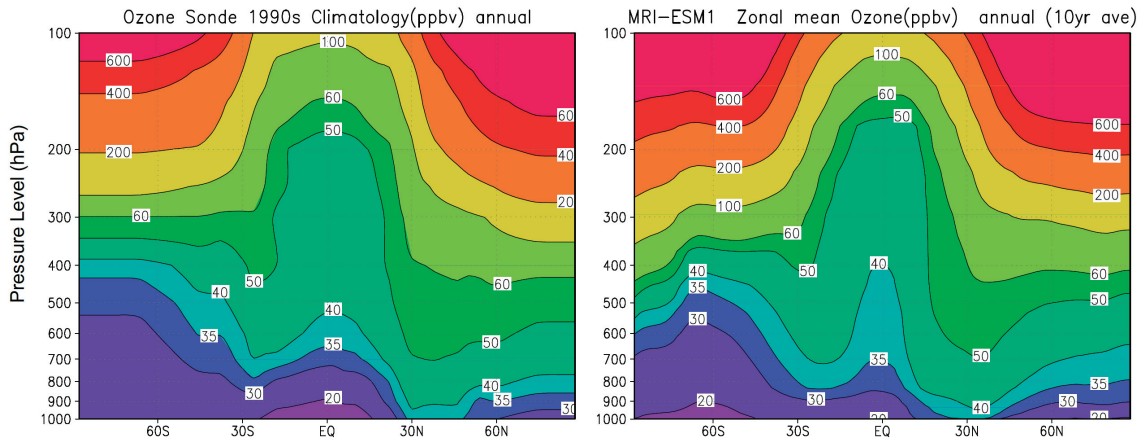


Figure 13 Annually averaged zonal-mean ozone mixing ratios (in ppbv) in the troposphere for sonde observation compiled by Logan (1999) (left) and the 1990s climatology of the MRI-ESM1 simulation (right).